Figure S1, Imoto, et al.

A

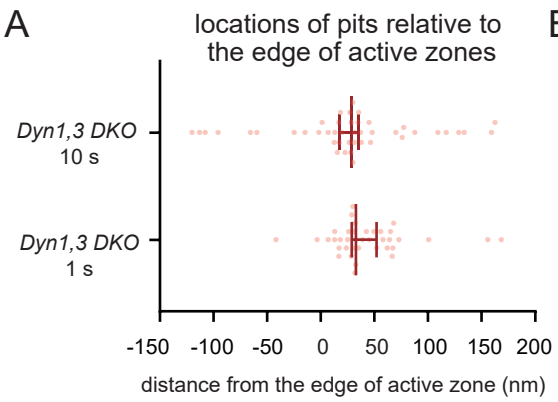

B

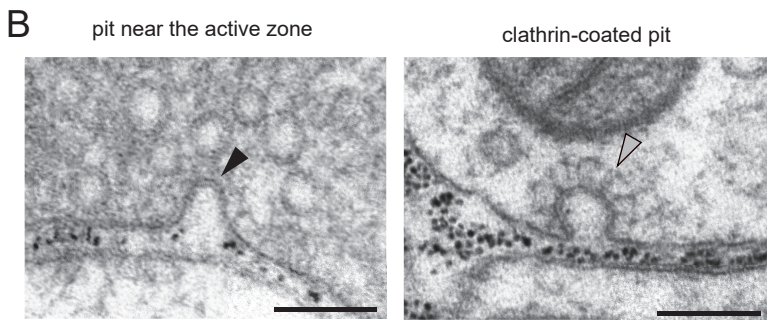

C

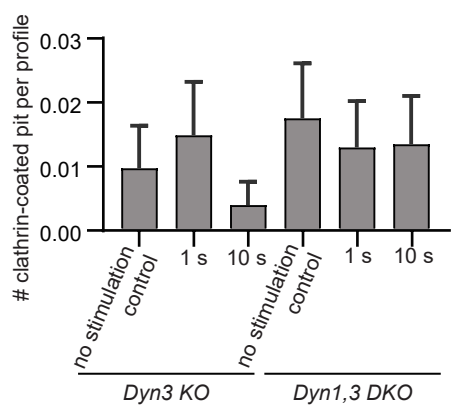

D

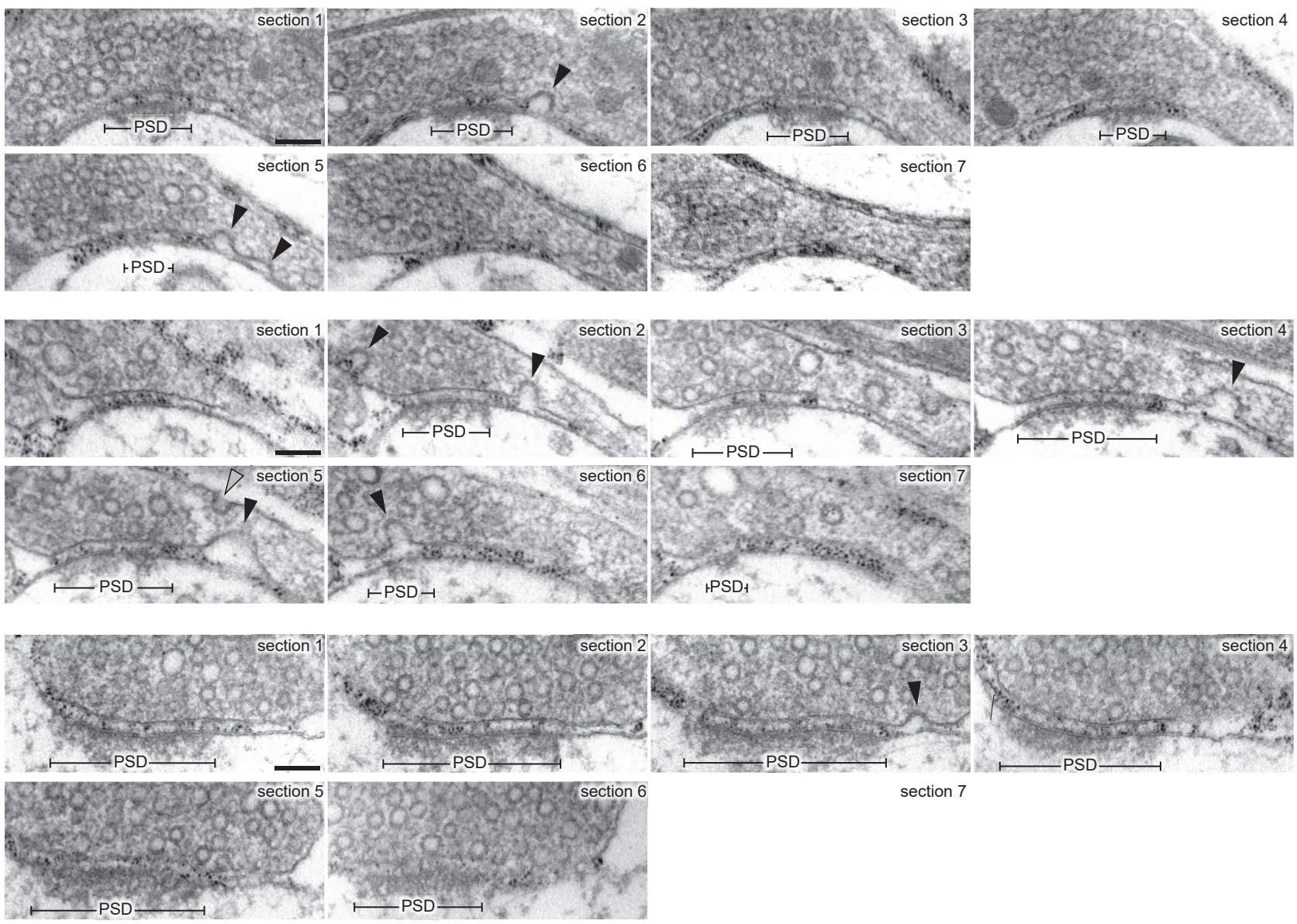

E

Figure S1. Endocytic pits in *Dyn1, 3* DKO neurons reconstructed from serial electron micrographs. Related to Figure 1.

(A) Locations of endocytic pits relative to the edge of an active zone. Each dot represents a pit. The negative and positive values indicate inside and out the active zone, respectively. The active zone is defined as the presynaptic membrane area juxtaposed to the postsynaptic density. The median and 95% confidence interval are shown. n = 57 pits for 1 s and 44 pits for 10 s. p = 0.2707. Mann-Whitney test was used. The same dataset as Figure 1.

(B) Example transmission electron micrographs showing endocytic pits and clathrin-coated pit structures in *Dyn1, 3* DKO neurons. Scale bar: 100 nm. Black arrowheads, endocytic invaginations. Clear arrowheads, clathrin-coated pit.

(C) Number of clathrin-coated pits in no stimulation control, at 1 s and at 10 s after stimulation. The numbers between *Dyn 3* KO and *Dyn1,3* DKO were not different, Ordinary one-way ANOVA with full pairwise comparisons by Tukey's multiple comparisons test. The mean and SEM are shown.

(D) Example transmission electron micrographs from serial sections of presynaptic terminals from Dyn1, 3 DKO neurons frozen 10 s after a single stimulus. Scale bar: 100 nm. PSD: post-synaptic density. Black arrowheads, endocytic invaginations. Translucent arrowheads, clathrin-coated pit.

(E) Graphical depictions of serial-sectioned bouton containing endocytic pits around active zones, from the experiments described in (D). The diameter of the depicted endocytic pits (black circle) reflects the width of the pit base.

Figure S2, Imoto, et al.

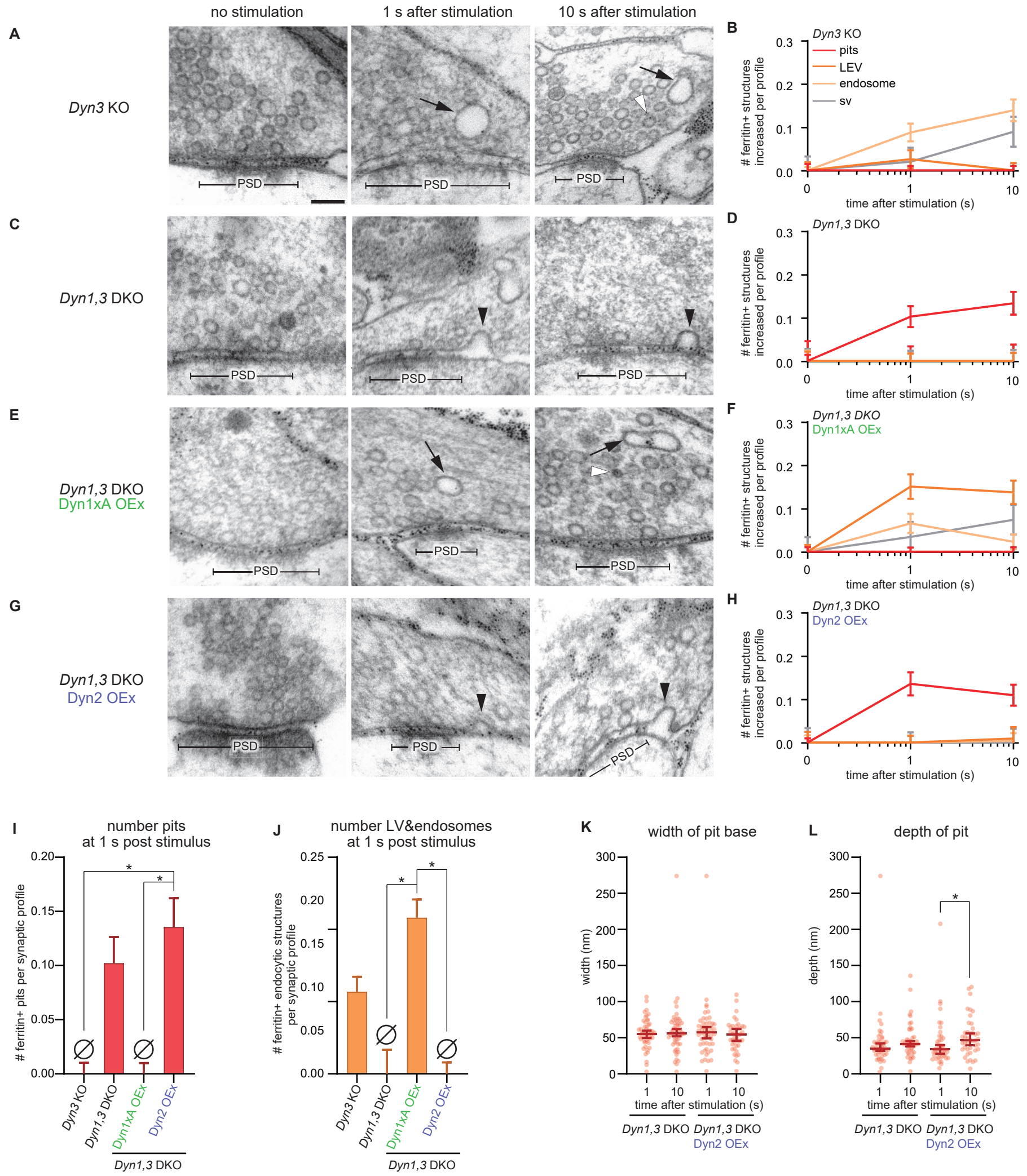

Figure S2. Overexpression of Dyn2 cannot rescue ultrafast endocytic defect of *Dyn1,3* DKO. Related to Figure 1.

(A, C, E and G) Example micrographs showing endocytic pits and ferritin-containing endocytic structures at the indicated time points in *Dyn3* KO neurons (A), *Dyn1, 3* DKO neurons (C), *Dyn1, 3* DKO neurons, overexpressing Dyn1xA (Dyn1xA OEx) (E) and *Dyn1, 3* DKO neurons, overexpressing Dyn2 (Dyn2 OEx) (G). Black arrowheads, endocytic pits; black arrows, ferritin-positive large endocytic vesicles (LEVs) or endosomes; white arrowheads, ferritin-positive synaptic vesicles. Note that Dyn2 OEx did no rescue the endocytic defect of *Dyn1, 3* DKO. Scale bar: 100 nm. PSD, post-synaptic density.

(B, D, F and H) Plots showing the increase in the number of each endocytic structure per synaptic profile after a single stimulus in *Dyn3* KO neurons (B), *Dyn1, 3* DKO neurons (D), *Dyn1, 3* DKO, Dyn1xA OEx neurons (F) and *Dyn1, 3* DKO, Dyn2 OEx neurons (H). The mean and SEM are shown in each graph.

(I) Number of endocytic pits at 1 s after stimulation. The numbers are re-plotted as a bar graph from the 1 s time point in (B, D, F and H) for easier comparison between groups. $p = 0.0455$ for *Dyn3* KO and 0.0455 for Dyn1xA OEx against Dyn2 OEx. Ordinary one-way ANOVA with full pairwise comparisons by Holm-Šídák's multiple comparisons test. The mean and SEM are shown.

(J) Number of ferritin-positive LEVs and endosomes at 1 s after stimulation. The numbers of LEVs and endosomes are summed from the data presented in (B, D, F and H), averaged, and re-plotted for easier comparison between groups. $p = 0.0205$ for *Dyn3* KO and 0.0205 for Dyn2 OEx against Dyn1xA OEx. Ordinary one-way ANOVA with full pairwise comparisons by Holm-Šídák's multiple comparisons test. The mean and SEM are shown.

(K and L) Plots showing the width (K) and depth (L) of endocytic pits at the 1s time point. The median and 95% confidence interval are shown in each graph. n = *Dyn1, 3* DKO, 51 pits for 1 s and 56 pits for 10 s; Dyn2 OEx, 52 pits for 1 s and 42 pits for 10 s. The depth: $p = 0.0475$ for Dyn2 OEx for 10 s against Dyn2 OEx for 1 s. Kruskal-Wallis Test with full comparisons by post hoc Dunn's multiple comparisons tests.

All data are from two independent experiments from N = 2 cultures prepared and frozen on different days. n = *Dyn* 3KO, 636; *Dyn1, 3* DKO, 631; *Dyn1, 3* DKO, Dyn1xA OEx, 617; and *Dyn1, 3* DKO, Dyn2, 600 synaptic profiles in (B, D, F, H, J, K, and L). *$p < 0.05$. See Quantification and Statistical Analysis for the n values and detailed numbers for each time point. Knock out neurons are from the littermates in all cases.

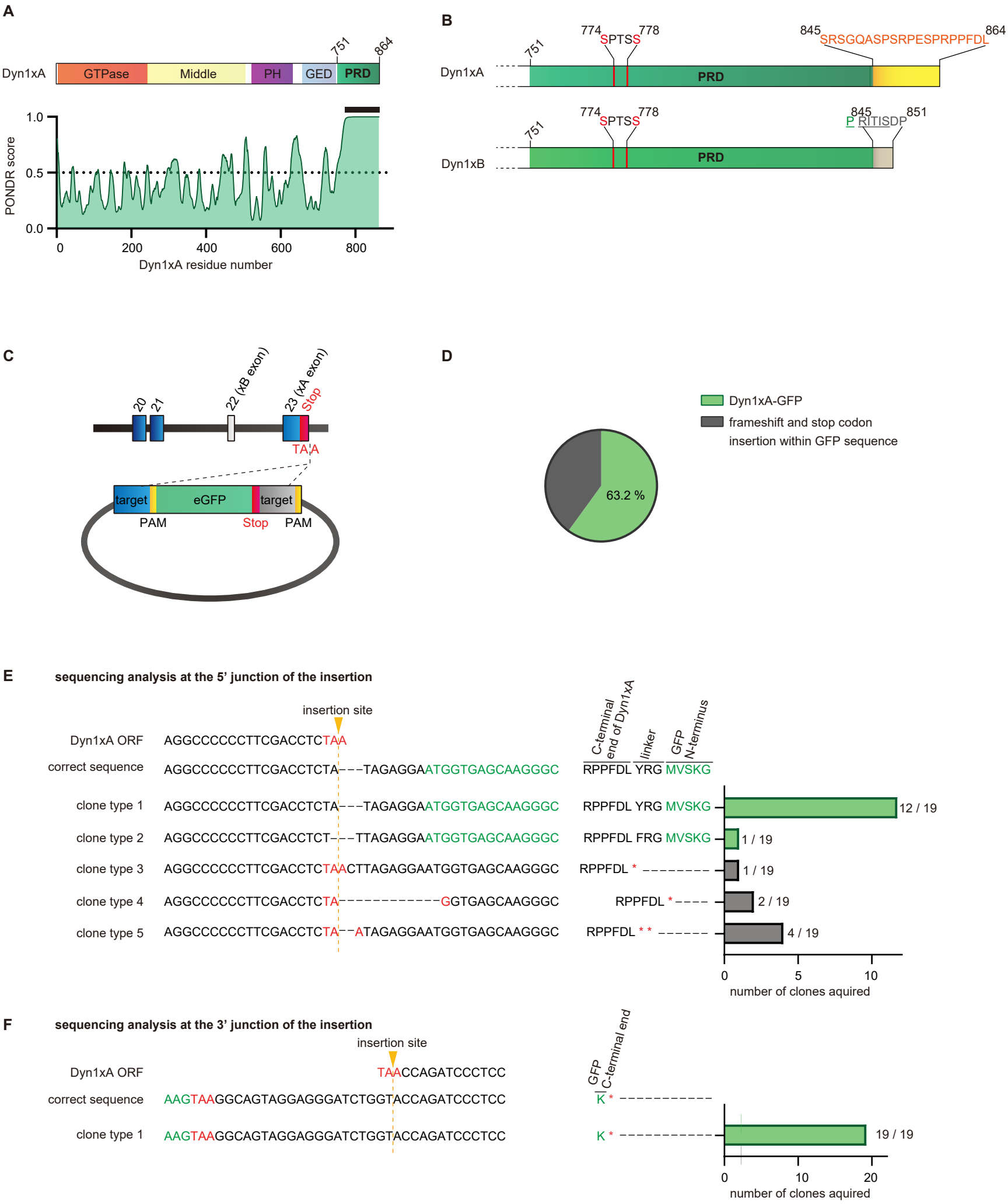
A
Dyn1xA
GTPase
Middle
PH
GED
PRD
751
864
PONDR score
1.0
0.5
0.0
0
200
400
600
800
Dyn1xA residue number
B
Dyn1xA
751
774
SPTSS
778
845
SRSGQASPSRPESPRPPFDL
864
PRD
Dyn1xB
751
774
SPTSS
778
845
P RITISDP
851
PRD
C
20
21
22 (xB exon)
23 (xA exon)
Stop
TAA
target
eGFP
target
PAM
Stop
PAM
D
Dyn1xA-GFP
frameshift and stop codon
insertion within GFP sequence
63.2 %
E
sequencing analysis at the 5' junction of the insertion
insertion site
C-terminal end of Dyn1xA
linker
GFP N-terminus
Dyn1xA ORF
AGGCCCCCCTTCGACCTCTAA
correct sequence
AGGCCCCCCTTCGACCTCTA---TAGAGGAATGGTGAGCAAGGGC
RPPFDL YRG MVSKG
clone type 1
AGGCCCCCCTTCGACCTCTA---TAGAGGAATGGTGAGCAAGGGC
RPPFDL YRG MVSKG
12 / 19
clone type 2
AGGCCCCCCTTCGACCTCT---TTAGAGGAATGGTGAGCAAGGGC
RPPFDL FRG MVSKG
1 / 19
clone type 3
AGGCCCCCCTTCGACCTCTAACTTAGAGGAATGGTGAGCAAGGGC
RPPFDL * --------
1 / 19
clone type 4
AGGCCCCCCTTCGACCTCTA----------GGTGAGCAAGGGC
RPPFDL * ----
2 / 19
clone type 5
AGGCCCCCCTTCGACCTCTA--ATAGAGGAATGGTGAGCAAGGGC
RPPFDL * * ------
4 / 19
0
5
10
number of clones aquired
F
sequencing analysis at the 3' junction of the insertion
insertion site
Dyn1xA ORF
TAACCAGATCCCTCC
correct sequence
AAGTAAGGCAGTAGGAGGGATCTGGTACCAGATCCCTCC
clone type 1
AAGTAAGGCAGTAGGAGGGATCTGGTACCAGATCCCTCC
GFP C-terminal end
K *
K *
19 / 19
0
10
20
number of clones aquired

Figure S3. 2D protein structures of Dyn1 and Sequencing analysis of CRISPR knock-in Dyn1xA. Related to Figure 2.

(A) A schematic showing the protein structural elements of Dyn1xA (top) and output of intrinsic disorder prediction program PONDR (http://www.pondr.com) for Dyn1xA (bottom). Dyn1xA contains the GTPase domain, the middle domain, the Pleckstrin homology (PH) domain, GTPase effector (GED) domain and Proline-rich domain (PRD). Only the PRD is the intrinsic disordered within Dyn1xA. An output of intrinsic disorder prediction program PONDR (http://www.pondr.com) for Dyn1xA (bottom).

(B) A schematic showing the C-terminus of Dyn1xA and Dyn1xB. Both splice variants share S774/778 phosphorylation sites. Dyn1xA contains a 20 amino acid extension at the end of the C-terminus (yellow), whereas Dyn1xB has a calcineurin binding motif (PxIxIS) at the C-terminus (grey). P844 is shown in green. The calcineurin binding motif is underlined.

(C) Schematics showing the knock-in strategy for tagging Dyn1xA at the endogenous locus with GFP in primary cultured hippocampal neurons. The gene structure of Dyn1 (top) and the schematic of the knock-in construct (bottom) are shown. eGFP was inserted into the stop codon after the xA exon.

(D) The proportion of successful Dyn1xA-GFP knock-in neurons.

(E) Sequencing analysis at the 5' junction of the insertion site. The following sequences are shown: nucleotide sequences of the Dyn1xA open reading frame (ORF), an expected sequence after the CRISPR based knock-in (correct sequence), and 5 different clones acquired from cultured cortical neurons infected with virus containing the CRISPR knock-in construct. The number of each clone acquired is summarized on the left. Clone type 1; the expected sequence. Clone type 2; only 1 amino acid was substituted in the linker peptide between Dyn1xA and GFP. Clone types 3-5; codon shifts, causing a stop codon insertion after the Dyn1xA ORF.

(F) Sequencing analysis at the 3' junction of the insertion site. Only the correct clone was obtained from cultured cortical neurons infected with virus containing the CRISPR knock-in construct. The experiment was performed from the same neurons in (A).

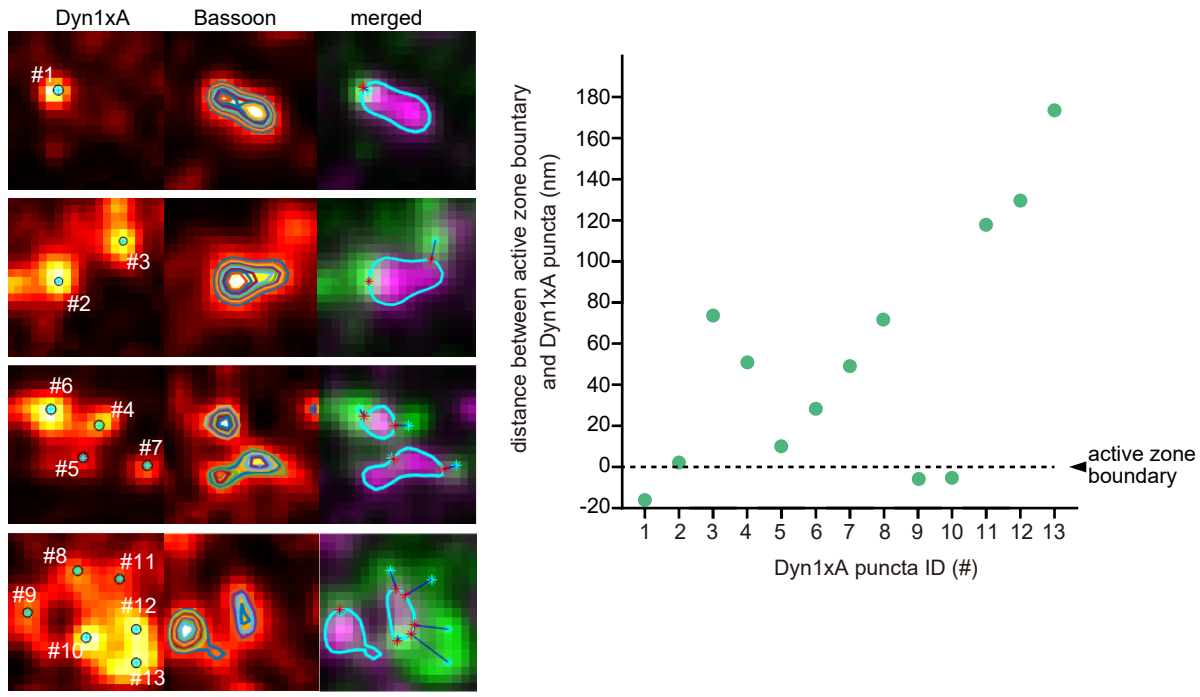
A
Dyn1xA
Bassoon
merged
#1
#2
#3
#4
#5
#6
#7
#8
#9
#10
#11
#12
#13
B
distance between active zone bountary and Dyn1xA puncta (nm)
180
160
140
120
100
80
60
40
20
0
-20
active zone boundary
1 2 3 4 5 6 7 8 9 10 11 12 13
Dyn1xA puncta ID (#)
C
+500 μg/mL digitonin
Dyn1xA
1 μm
mC-Syb2
0 s
10 s
20 s
30 s
40 s
50 s
60 s
4.0
1.0
D
+500 μg/mL digitonin
Dyn1xA (puncta)
Dyn1xA (cytosolic)
mC-Syb2
normalized fluorescence
1.5
1.0
0.5
0.0
-20 -10 0 10 20 30 40 50 60
time (s)
E
normalized fluorescence 60 s after the digitonin addition
1.5
1.0
0.5
0.0
*
**
Dyn1xA (puncta)
Dyn1xA (cytosolic)
mC-Syb2
F
fusion
Dyn1xA
0 s
5 s
10 s
15 s
20 s
25 s
30 s
35 s
500 nm
fission
Dyn1xA
0 s
5 s
10 s
15 s
20 s
25 s
30 s
35 s
500 nm

Figure S4. Analysis of Dyn1xA localization in neurons. Related to Figure 2.

(A) Example STED images showing automatic segmentation of Dyn1xA and Bassoon signals with MATLAB codes. Dyn1xA was stained with anti-GFP antibodies and αBassoon was stained with anti-Bassoon antibodies. Dots #1-#13 in Dyn1xA channel indicate local maxima of Dyn1xA puncta. The outermost concentric circle in the Bassoon channel (middle) indicates the active zone boundary and is defined by 0.5-fold local maxima of the Bassoon signal. In merged images, the local maxima of Dyn1xA puncta are shown as light blue asterisks, and active zone boundaries are shown as light blue lines. Nearest distance between the local maxima of Dyn1xA puncta and the active zone boundaries are connected with blue lines. See Material & Method section for more detail analysis protocol and MATLAB scripts.

(B) Plots showing the distance of each Dyn1xA punctum from its local maximum to the nearest active zone boundary. Numbers on x-axis correspond to dots #1-#13 in (A).

(C) Example live-cell fluorescence micrographs showing overexpression of Dyn1xA and mCherry-Syb2 (mC-Syb2) before and after the digitonin treatment. Time indicates after the 500 μg/mL of digitonin addition. Images are false-colored to indicate relative intensity.

(D) Averaged normalized fluorescence intensities of Dyn1xA puncta, cytosolic Dyn1xA and mC-Syb2 before and after the digitonin addition along the time course. Fluorescence is normalized to the pre-treatment. To define puncta, Gaussian smoothing ($\sigma = 0.2$) was applied on images, and the signals below the average fluorescence intensity of Dyn1xA or Syb2 in the intersynaptic axonal regions removed. The resulting puncta were delineated and set as ROIs. Dyn1xA puncta were defined the puncta adjusting or within Syb2 signals. Any signals outside the Dyn1xA ROIs and around Syb2 signals are defined as cytosolic Dyn1xA. The median and 95% confidence interval are shown.

(E) Fluorescence intensities of Dyn1xA puncta, cytosolic Dyn1xA within presynaptic boutons, and mC-Syb2, re-plotted from the 60 s time point in (B). The median and 95% confidence interval are shown in each graph. p = 0.0008 for cytosolic Dyn1xA and 0.0188 for mC-Syb2 against Dyn1xApuncta. Kruskal–Wallis tests with comparisons against Dyn1xA by post hoc Dunn's multiple comparisons tests.

For (C-E), 17 different presynapses in 3 different neurons were examined from 2 independent cultures.

(F) Example live cell images showing Dyn1xA puncta undergoing fusion (top) and fission (bottom) events. Times after the initiation of image acquisitions are indicated.

N = 2 or more independent cultures. *p < 0.05, **p < 0.0001. See Quantification and Statistical Analysis for the n values and detailed numbers.

Figure S5, Imoto, et al.

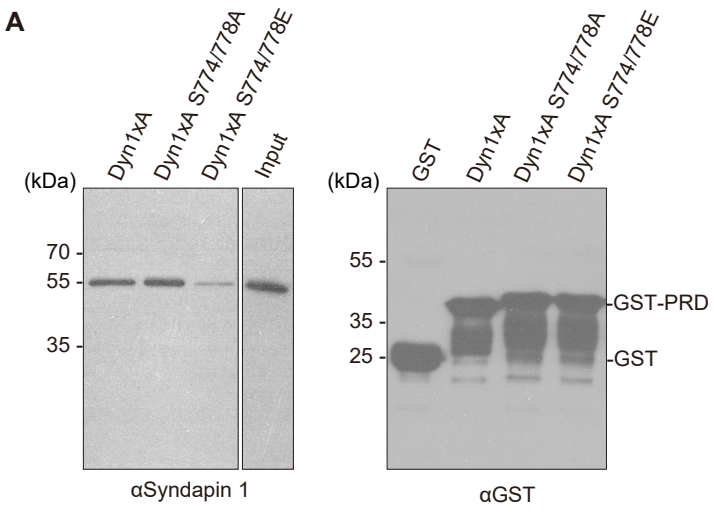

Figure S5. *in vitro* phase separation assay of Dyn1xA and Syndapin1. Related to Figure 3.

(A) Immunoblotting images showing a GST pull-down assay of the recombinant PRM of Dyn1xA, Dyn1xA S774/778A or Dyn1xA S774/778E and anti-Syndapin 1 antibody reactions. The assay was performed using the lysate of synaptosome fractions isolated from adult mouse whole brains. Right blot showing the blotting against anti-GST antibody used for normalization of signals in left blot.

(B) Normalized signal intensities of Syndapin 1 acquired from the immunoblotting using Dyn1xA PRM constructs shown in (J). Signal intensities were normalized to the amount of GST-PRMs .The median and 95% confidence interval are shown.

(C) Purities of recombinant proteins used in this study. Wild-type Dyn1xA (Dyn1xA wt), Dyn1xA S774/778D, wild-type Syndapin1 (Syndapin1 wt) and Syndapin1 P434L were purified from bacteria (see Material and Method) and assessed by SDS-PAGE and Gel code staining.

(D) Dyn1xA and Syndapin1 droplet formation at various protein concentrations. Enlarged images are shown in the insets.

(E) Syndapin1 droplets at various concentrations of protein and salt.

(F) Syndapin1 droplets with or without 5% PEG.

(G) Dyn1xA and Syndapin1 droplets with or without 2.5% or 5% PEG.

(H) Dyn1xA (2 μM) or Syndapin 1 (20 μM) were examined by sedimentation assay with or without 5 % PEG. The supernatant (S) and pellet (P) were collected by centrifugation at ×13,000 rpm for 10 min, and then proteins were subjected to SDS−PAGE and Gel code staining.

(I, J) Pellet fraction of Dyn1xA (F) and Syndapin1 (G) calculated from protein bands in supernatants and pellet fractions in (E). *, $P < 0.05$. **, $P < 0.001$. Mean ± SEM are shown. $n = 4$ from two independent protein purification.

(K) Normalized fluorescence intensity from the FRAP experiments in Figure 1C, showing the fluorescence is in the linear range of the detection.

$N = 3$ from different mouse brains in all cases. * $p < 0.05$. See Quantification and Statistical Analysis for the n values and detailed numbers.

(L) Example images of purified Dyn1xA S774/778D (labeled with Alexa488) and Syndapin1 (labeled with Alexa 549), or Dyn1xA (labeled with Alexa488) and Syndapin1 P434L (labeled with Alexa 549) under physiological salt concentration and with 5 % PEG.

All data are examined by $n > 15$ droplets from two independent protein purifications.

(M) Schematics represents low-speed sedimentation assay.

(N) Dyn1xA (2 μM) and Syndapin 1 (10 μM) were used with and without 5 % PEG. The supernatant (S) and pellet (P) were collected by centrifugation at ×13,000 rpm for 10 min and then proteins were subjected to SDS−PAGE and Gel code staining (I).

(O, P) The pellet fraction of Dyn1xA (I) and Syndapin1 (J) were calculated from protein bands in supernatants and pellet fraction in (H). *, $P < 0.05$. **, $P < 0.001$. Mean ± SEM are shown. $n = 4$ from two independent protein purification.

Figure S6, Imoto, et al.

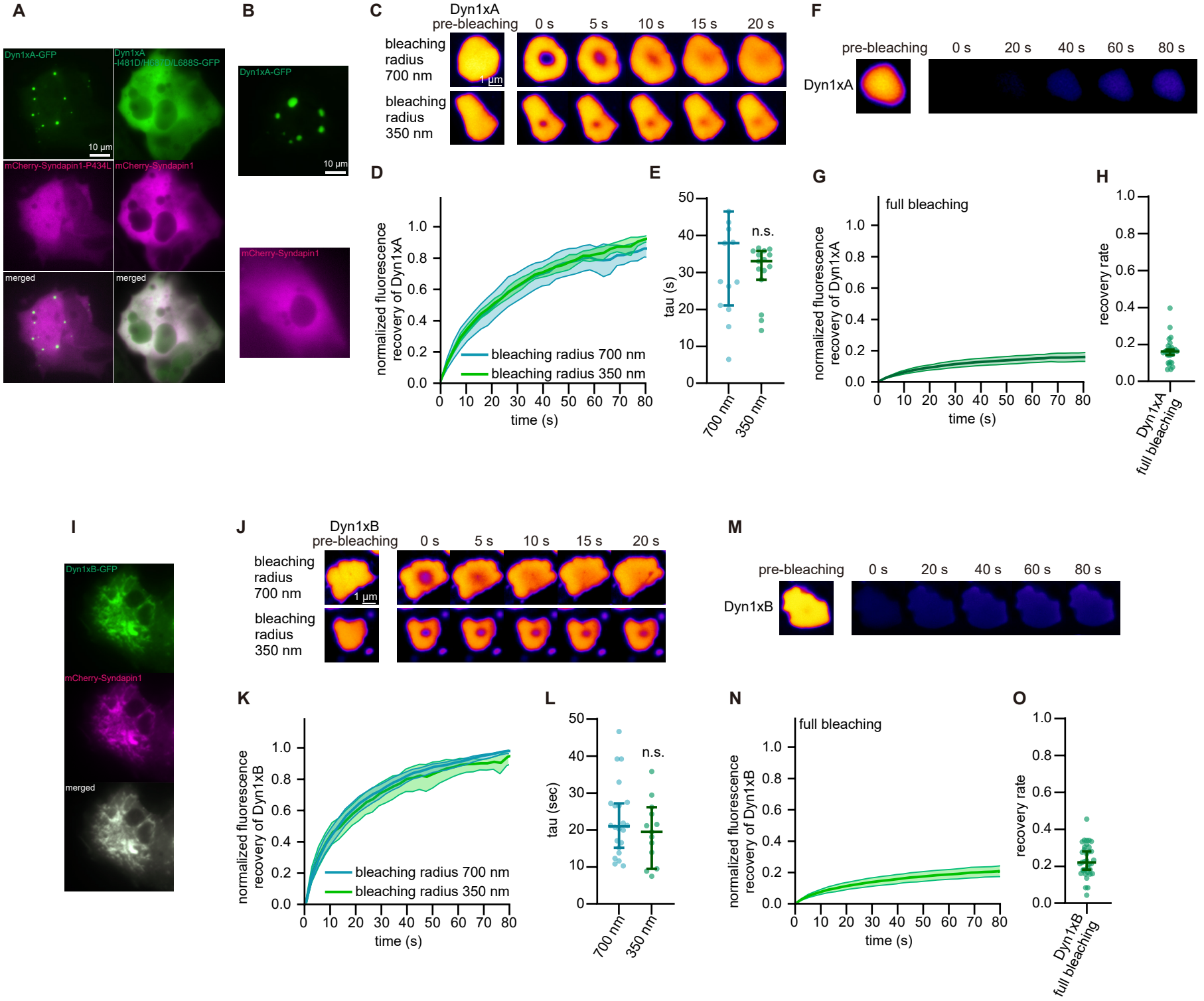

Figure S6. Phase separation assay of Dyn1xA and Syndapin1 in COS-7 cells. Related to Figure 3.

(A) Dyn1xA-GFP or Dyn1xA monomeric mutant (Dyn1xA-I481D/H637D/I688S)-GFP co-overexpressed in COS-7 cells with mCherry-Syndapin1 P434L or mCherry-Syndapin1 wild-type, respectively.

(B) Dyn1xA-GFP or mCherry-Syndapin1 expressed individually in COS-7 cells.

(C) Example time-lapse images of FRAP experiments inside of droplet-like Dyn1xA-GFP. Dyn1xA signals were photobleached at 480 nm using the ROI radius of 700 nm or 350 nm. Time indicates after the photobleaching.

(D) Normalized fluorescence recovery of Dyn1xA signals in the indicated ROI sizes. Fluorescence signals were normalized between immediately (0 s) and 80 s after the photobleaching. Times indicate after the photobleaching. The median and 95% confidential interval are shown.

(E) The recovery time constant of Dyn1xA signals following the photobleaching using different ROI sizes in (D). The median and 95% confidence interval are shown. Each dot represents a droplet-like structure of Dyn1xA. $p < 0.0001$. Mann-Whitney test.

(F) Examples time-lapse images of FRAP experiments on the Dyn1xA-GFP droplet-like structure with the photobleaching laser covering the entire structure. Dyn1xA signals were photobleached with 480-nm laser.

(G) Normalized fluorescence recovery of Dyn1xA signals. Fluorescence signals were normalized at immediately (0 s) and 80 s after the photobleaching. Times indicate after the photobleaching. The median and 95% confidential interval are shown.

(H) The recovery rate of Dyn1xA signals at 80s after the photobleaching in (G). The median and 95% confidence interval are shown. Each dot represents a droplet-like structure of Dyn1xA-GFP.

(I) Dyn1xB-GFP and mCherry-Syndapin1 co-expressed in COS-7 cells.

(J) Examples time-lapse images of FRAP experiments on Dyn1xB-GFP and mCherry-Syndapin1 droplet-like structures. Dyn1xB signals were photobleached with 480-nm laser using the ROI radius of 700 nm or 350 nm. Time indicates after the photobleaching.

(K) Normalized fluorescence recovery of Dyn1xB signals inside the photobleached spots. Fluorescence signals were normalized between immediately (0 s) and 80 s after the photobleaching. Times indicate after the photobleaching. The median and 95% confidential interval are shown.

(L) The recovery time constant of Dyn1xB signals following the photobleaching using the indicated ROI sizes. The median and 95% confidence interval are shown. Each dot represents a droplet-like structure of Dyn1xB-Syndapin1. n.s., no significance. Mann-Whitney test.

(M) Examples time-lapse images of FRAP experiments Dyn1xB-GFP and mCherry-Syndapin1 droplet-like structure of with the photobleaching laser covering the entire structure. Dyn1xB signals were photobleached with 480-nm laser.

(N) Normalized fluorescence recovery of Dyn1xB signals after the full bleaching. Fluorescence signals were normalized at just after (0 s) the photobleaching. Times indicate after the photobleaching. The median and 95% confidential interval are shown.

(O) The recovery rate of Dyn1xB signals at 80s after the photobleaching in (N). The median and 95% confidence interval are shown. Each dot represents a droplet-like structures of Dyn1xB-GFP and mCherry-Syndapin1.

n >15 droplets in more than 5 cells from 2 or 3 different cell preparations. See Quantification and Statistical Analysis for the n values and detailed numbers.

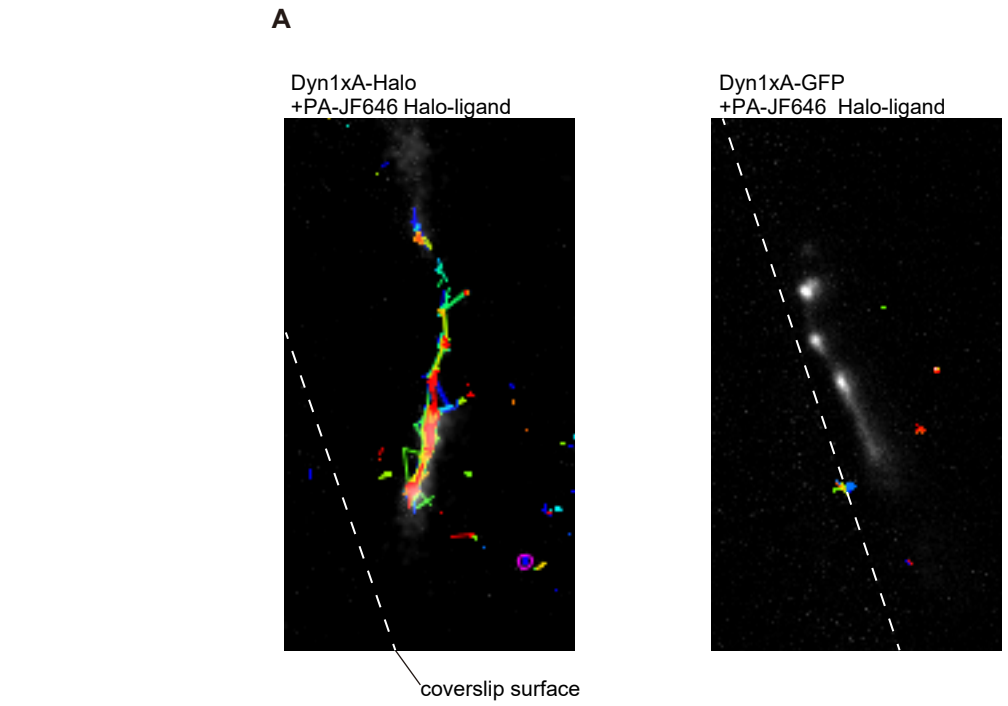
A
Dyn1xA-Halo
+PA-JF646 Halo-ligand
Dyn1xA-GFP
+PA-JF646 Halo-ligand
coverslip surface
B
neurons expressing Dyn1xA-Halo
800
600
400
200
a Dyn1xA molecule displacement (nm)
500 nm
mask for Dyn1xA puncta
neurons expressing Dyn1xA-GFP
800
600
400
200
a non-specific PA-JF646 molecule displacement (nm)
C
dwelling
crossing
D
entire trajectories crossing boundary of the puncta
entire trajectories dwelling inside the puncta
E
D1 (slow)
D2 (intermediate)
D3 (free diffusion)
diffusion coefficient (μm2/s)
1×10^0
1×10^-1
1×10^-2
crossing + dwelling
crossing
dwelling
F
D1 (slow)
D2 (intermediate)
D3 (free diffusion)
fraction
0.6
0.4
0.2
0.0
crossing + dwelling
crossing
dwelling

Figure S7. Phase separation assay of Dyn1xA puncta in neurons. Related to Figure 4.

(A) Example tracking maps of photoactivated PA-JF646-halo ligands in neurons expression Dyn1xA-Halo or Dyn1xA-GFP. Dashed lines show cover slip surface.

(B) Example localization maps of photoactivated Dyn1xA molecules in boutons with Dyn1xA punctum in neurons expressing Dyn1xA-Halo (Top panel, total 27699 molecules are detected in 88 boutons). And non-specific binding of photoactivated PA-JF646-halo ligands in neurons expressing Dyn1xA-GFP (bottom panel, total 50 molecules are detected in 49 bouton). The color histogram indicates the displacement distance of each Dyn1xA molecule.

(C) Schematic showing entire trajectories of molecules crossing the boundary or those staying inside the puncta (dwelling).

(D) Example entire trajectories of crossing and dwelling molecules depicted by the Matlab scripts. These trajectories are used for calculation of diffusion coefficient in Figure 4P-R.

(E) Diffusion coefficient of three components in Figure 4P-R. $n > 150$ iterations.

(F) Fraction of diffusion coefficient of three components in Figure 4P-R. $n > 150$ iterations.

Figure S8, Imoto, et al.

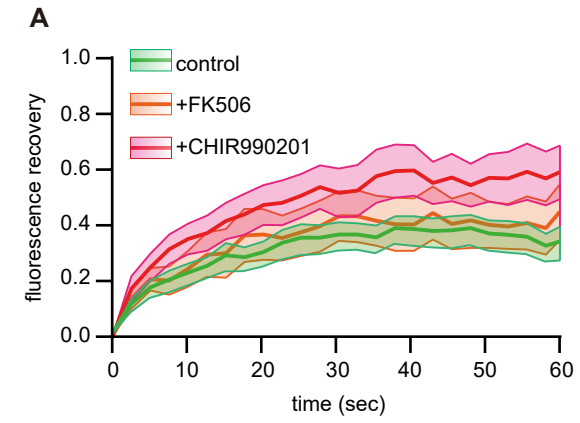

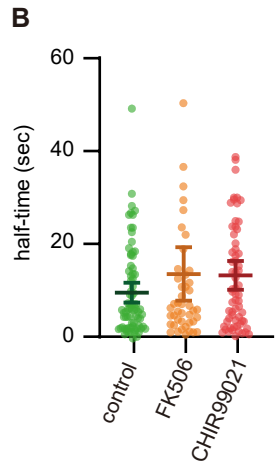

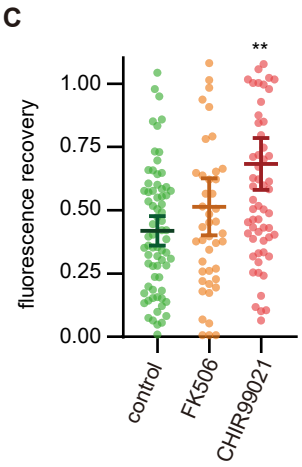

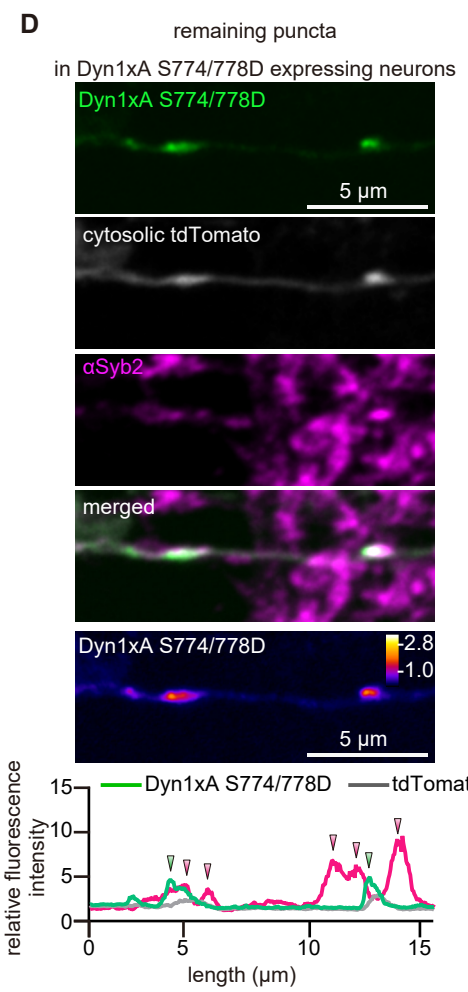

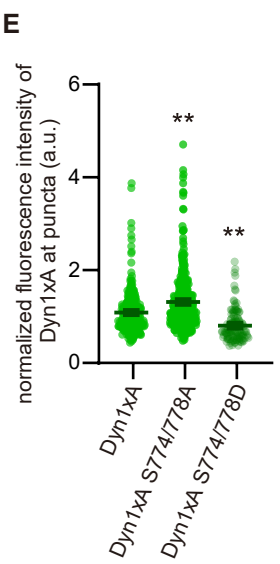

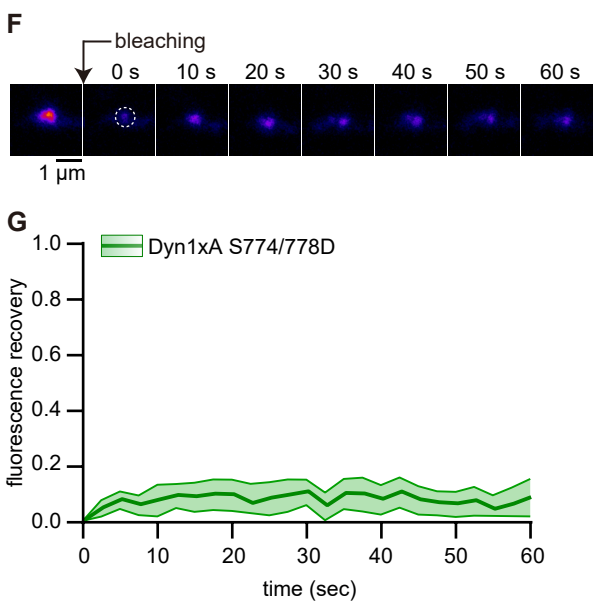

Figure S8. Dephosphorylation of PRD regulates formation of Dyn1xA puncta. Related to Figure 5.

(A) Fluorescence recovery of Dyn1xA signals in DMSO (control), calcineurin inhibitor (FK506) or GSK3β inhibitor (CHIR99021) treated neurons. The entire puncta of Dyn1xA were photobleached in each case, and the recovery measured. The median and 95% confidence interval are shown.

(B) Plots showing the half-time of Dyn1xA signals in the indicated conditions: control, FK506, CHIR99021. The median and 95% confidence interval are shown. The half-time is calculated at the recovery period of 60 s after photobleaching. The median and 95% confidence interval are shown. Each dot represents a punctum. The number was not different between the conditions. Kruskal–Wallis tests with comparisons against Dyn1xA by post hoc Dunn's multiple comparisons tests.

(C) Plots showing the fraction of fluorescence recovery 60 s after photobleaching of the entire Dyn1xA puncta in control, FK506, and CHIR99021-treated neurons. The median and 95% confidence interval are shown. Each dot represents a punctum. $p = 0.0003$ for CHIR99021 against control. Kruskal–Wallis tests with comparisons against Dyn1xA by post hoc Dunn's multiple comparisons tests.

n = Dyn1xA puncta, 71; FK506, 46; and CHIR99021, 64 in (A-C). At least 4 different neurons were examined from 2 independent cultures. The Dyn1xA puncta data are shared with Figure 3B-D. FK506 and CHIR99021 experiments were used same cultures as in Figure 3B-D.

(D) Example confocal immunofluorescence micrographs showing the overexpression of Dyn1xA S774/778D along with exogenously expressed cytosolic tdTomato and immuno-stained αSyb2. False-colored images show the relative fluorescence intensity of Dyn1xA S774/778D. Line scan graphs represent the localization of Dyn1xA S774/778D relative to cytosolic tdTomato and αSyb2.

(E) Normalized fluorescence intensities of Dyn1xA, Dyn1xA S774/778A or Dyn1xA S774/778D puncta. n = 287 puncta in Dyn1xA, 373 puncta in Dyn1xA S774/778A, and 123 puncta in Dyn1xA S774/778D from 2 separate cultures. The median and 95% confidence interval are shown. $p < 0.0001$ for Dyn1xA S774/778A and for Dyn1xA S774/778D against Dyn1xA. Kruskal–Wallis tests with comparisons against Dyn1xA by post hoc Dunn's multiple comparisons tests.

The same data as in Figure 4 was analyzed.

(F) Examples live images of FRAP experiments of Dyn1xA-S774/778D-GFP puncta in presynapse. Dyn1xA-S774/778D-GFP signals were photobleached at 480 nm. Time indicates after the photobleaching.

(G) Normalized fluorescence recovery of Dyn1xA-S774/778D-GFP signals. Fluorescence signals were normalized to just after (0 s) photobleaching. Times indicate after the photobleaching. The median and 95% confidential interval are shown.

Figure S9, Imoto, et al.

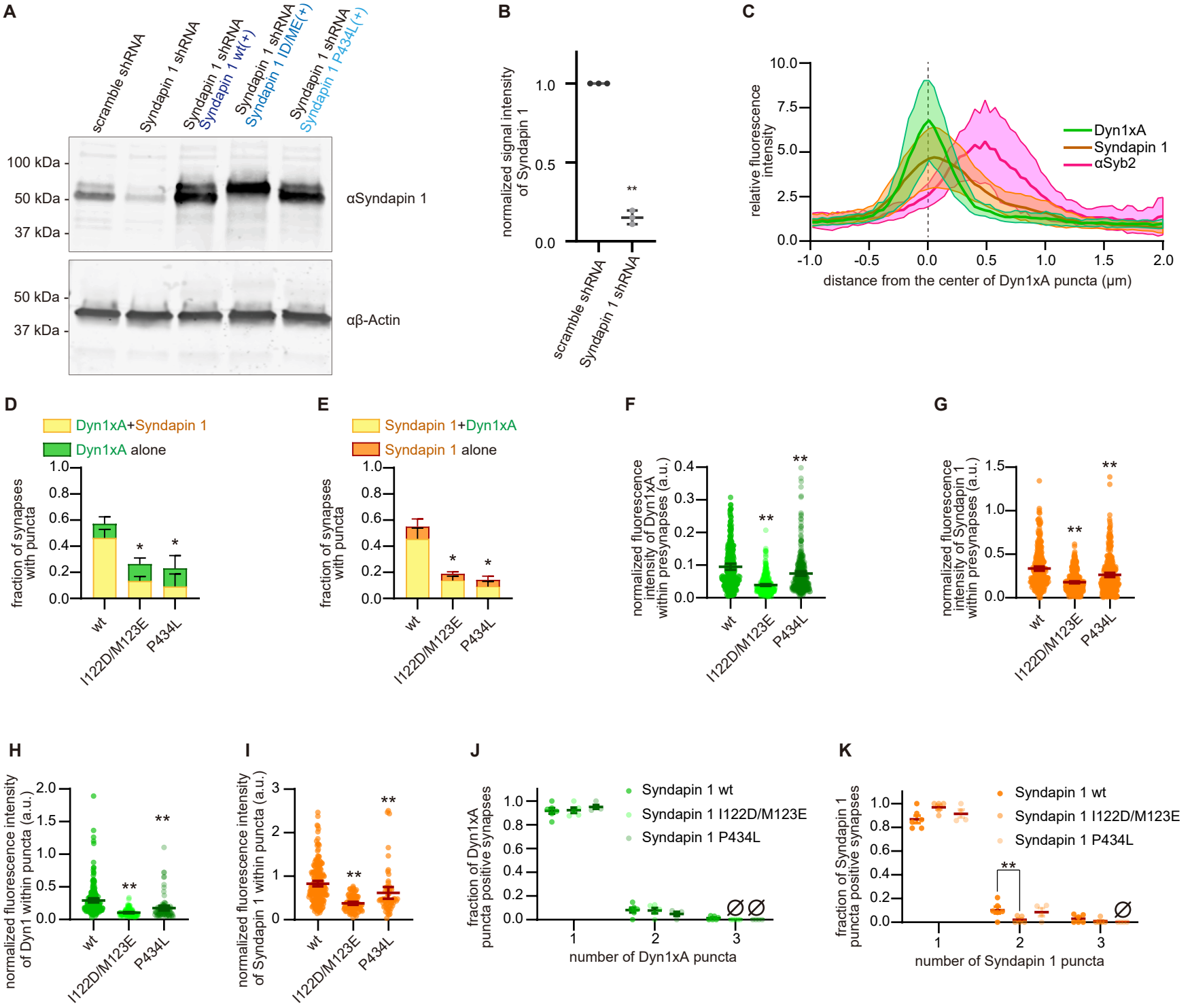

Figure S9. Syndapin 1 is essential for the localization of Dyn1xA. Related to Figure 7.

(A) Immunoblotting images showing anti-Syndapin 1 or anti-β-Actin antibodies reactions against the lysates of cultured hippocampal neurons infected with lentivirus expressing scramble shRNA, Syndapin 1 shRNA, Syndapin 1 shRNA and Syndapin 1 wild type (wt) (+), Syndapin 1shRNA + Syndapin 1 I122D/M123E (ID/ME) (+) or Syndapin 1shRNA + Syndapin 1 P434L (+).

(B) Normalized signal intensities of Syndapin 1 in immunoblotting assays using neurons expressing scramble shRNA or Syndapin shRNA. **$p < 0.0001$, unpaired t test. The mean and SEM are shown.

n = 3 independent cultures.

(C) The distribution of αSyb2 and wild-type Syndapin 1 relative to the peak of Dyn1xA signals. Line scans of fluorescence from 12 synapses, defined by the end-to-end Syb2 signals, were aligned based on the peak pixel of Dyn1xA signals, and fluorescence intensities averaged. The median and 95% confidence interval are shown.

(D) The fraction of synapses with Dyn1xA puncta that colocalize (yellow) or does not colocalize with Syndapin 1 (green) wild type (wt) or mutants (I122D/M123E, and P434L).

(E) The fraction of synapses with wild type (wt) or mutant (I122D/M123E, and P434L) Syndapin 1 puncta that colocalize (yellow) or does not colocalize with Dyn1xA puncta (orange).

(F and G) Normalized fluorescence intensities of Dyn1xA (F) and Syndapin 1 (G) within presynapses of neurons expressing wild-type or mutant (I122D/M123E, and P434L) Syndapin 1. Each dot represents a presynapse. n = 332 for wt, 418 for I122D/M123E, and 341 for P434L. Dyn1xA intensities; $p = < 0.0001$ for I122D/M123E and 0.0004 for P434L against Syndapin 1 expressing neurons. Syndapin 1 intensities; $p = < 0.0001$ for I122D/M123E and for P434L against wt expressing neurons. Kruskal–Wallis tests with comparisons against wt by post hoc Dunn's multiple comparisons tests. The median and 95% confidence interval are shown.

(H and I) Normalized fluorescence intensities of Dyn1xA puncta (H) and Syndapin 1 puncta (I) of neurons expressing wild-type or mutant (I122D/M123E and P434L) Syndapin 1. Each dot represents a punctum. Dyn1xA puncta: n = 208 for wt, 120 for I122D/M123E, and 91 for P434L. Syndapin 1 puncta: n = 202 for wt, 88 for I122D/M123E, and 60 for P434L. Dyn1xA intensities; $p = < 0.0001$ for I122D/M123E and for P434L against Syndapin 1 expressing neurons. Syndapin 1 intensities; $p = < 0.0001$ for I122D/M123E and for P434L against wt expressing neurons. Kruskal–Wallis tests with comparisons against wt by post hoc Dunn's multiple comparisons tests. The median and 95% confidence interval are shown.

(J and K) Relative frequency distributions of the number of Dyn1xA puncta (J) and Syndapin 1 puncta (K) within presynaptic boutons among those that contain at least one punctum in neurons expressing wild-type or mutant (I122D/M123E and P434L) Syndapin 1. The mean and SEM are shown in each graph. The fraction is calculated from each neuron. The mean and SEM are shown. n = 6 for Syndapin 1 expressing neurons, 5 for I122D/M123E and 4 for P434L. P = 0.0095 for two

puncta per synapses in I122D/M123E against Syndapin 1 expressing neurons. Two way ANOVA with Šídák's multiple comparisons test.

> 50 boutons were quantified from at least 4 different neurons. N = 2 or more independent cultures. * $p < 0.05$, ** $p < 0.0001$. See Quantification and Statistical Analysis for the n values and detailed numbers.

Figure 10, Imoto, et al.

A The function of Dynamin during clathrin mediated-endocytosis

Phase 1
Clathrin and early endocytic proteins form membrane curvature.
Most of endocytic proteins including dynamin are diffuse in the cytosol

Phase 2
Dynamins and BAR proteins gradually accumulate and assemble into scaffold structures around the neck of endocytic pits

Phase 3
Assembled endocytic mechineries constrict the neck of pits, and vesicles are severed from the plasma membrane

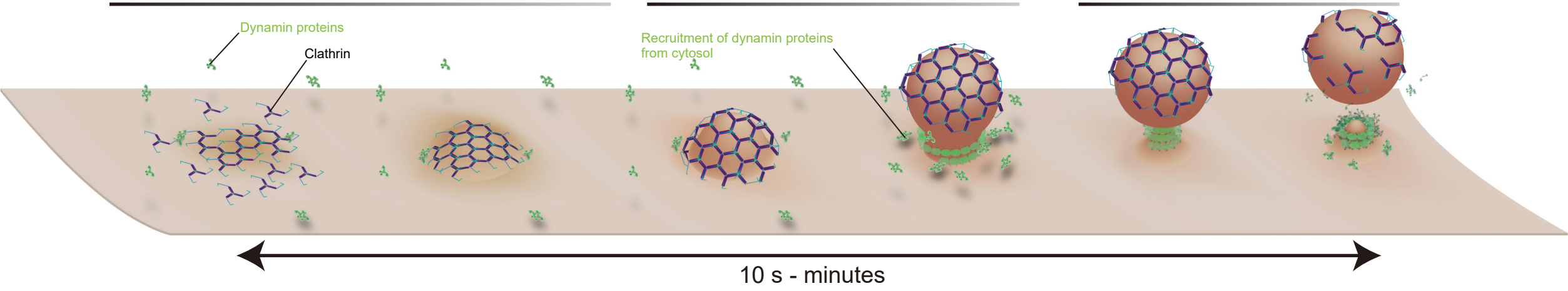

B A model of Dyn1xA and Syndapin 1 during ultrafast endocytosis

Phase 1
Synaptic vesicles fuse to plasma membrane upon neural stimulations. Membrane squeezes towards outside of active zone

Phase 2
Dyn1xA and Syndapin 1 are pre-recruited to the endocytic zone

Phase 3
Dyn1xA and Syndapin 1 assemble without the recruitment from the cytosol and drive membrane constriction

Phase 4
Dyn1xA constricts the neck, and vesicles are severed from the plasma membrane within 100 ms after stimulation

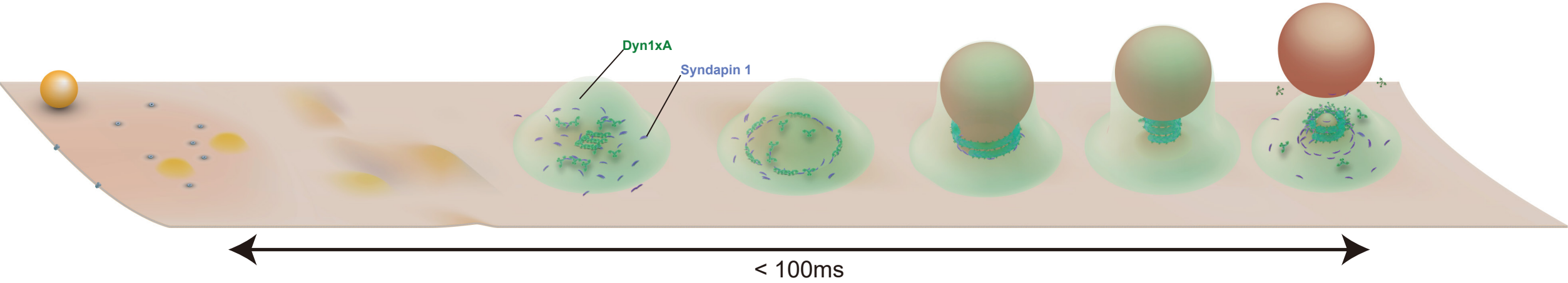

Multivalent weak hydrophobic interaction between Dyn1xA and Syndapin 1 leads to the liquid-like contensates

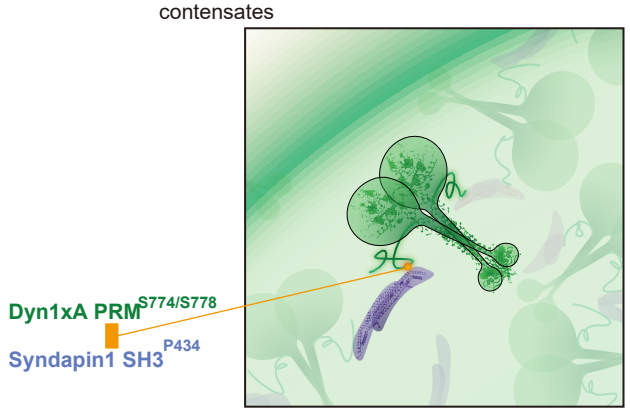

Dyn1xA are anchored to the membrane through the wedge loop of Syndapin 1

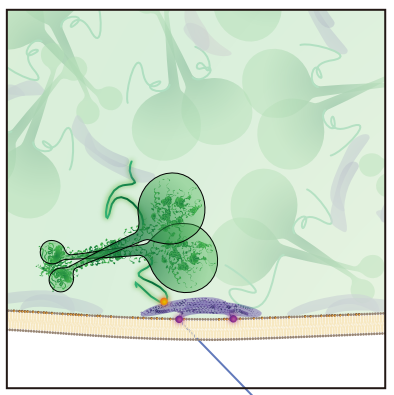

Figure S10. Schematics depicting the differences between clathrin-mediated endocytosis and ultrafast endocytosis. Related to Figure 1 - 8.

In clathrin-mediated endocytosis (A), dynamin and endocytic proteins are recruited from the cytosol. This process is slow, taking tens of seconds. For ultrafast endocytosis (B), the Dyn1xA splice variant forms phase-separated puncta within presynaptic boutons. The puncta are likely maintained through the multivalent interaction of Dyn1xA PRM with the SH3 domain of Syndapin 1. The puncta are anchored to the plasma membrane, just outside the active zone, through the wedge loop of Syndapin 1. Loss of interactions among these proteins or the membrane anchor of Syndapin 1 slows down the kinetics of ultrafast endocytosis by 100-fold, since these proteins become cytosolic and need to be recruited to the endocytic sites after the initiation of ultrafast endocytosis.

Figure S6, Imoto, et al.

Dyn3 KO

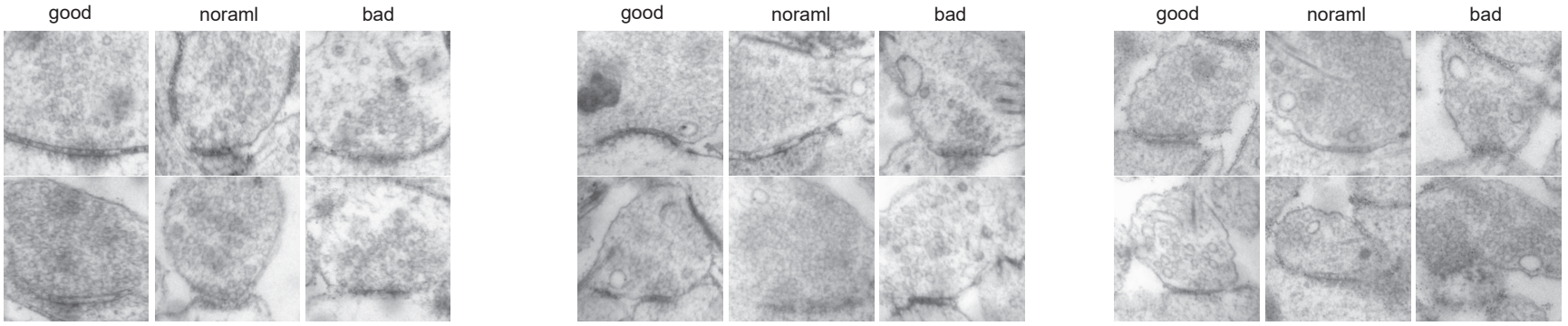

Dyn1,3 DKO

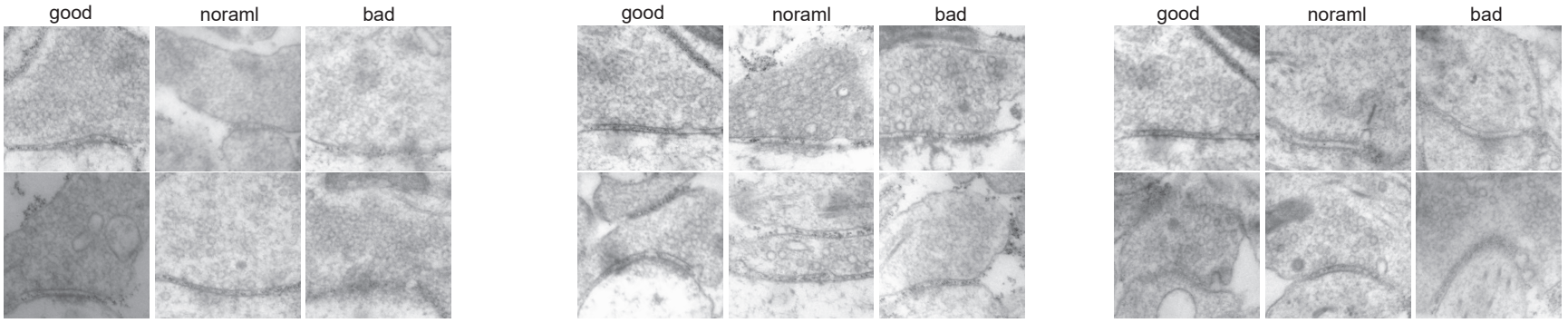

Dyn1,3 DKO
Dyn1xA OEx

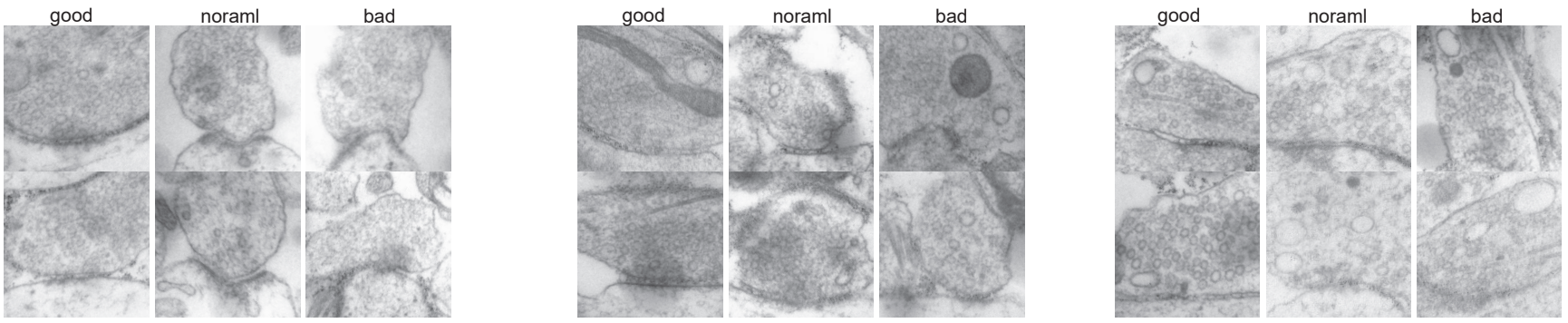

Dyn1,3 DKO
Dyn1xB OEx

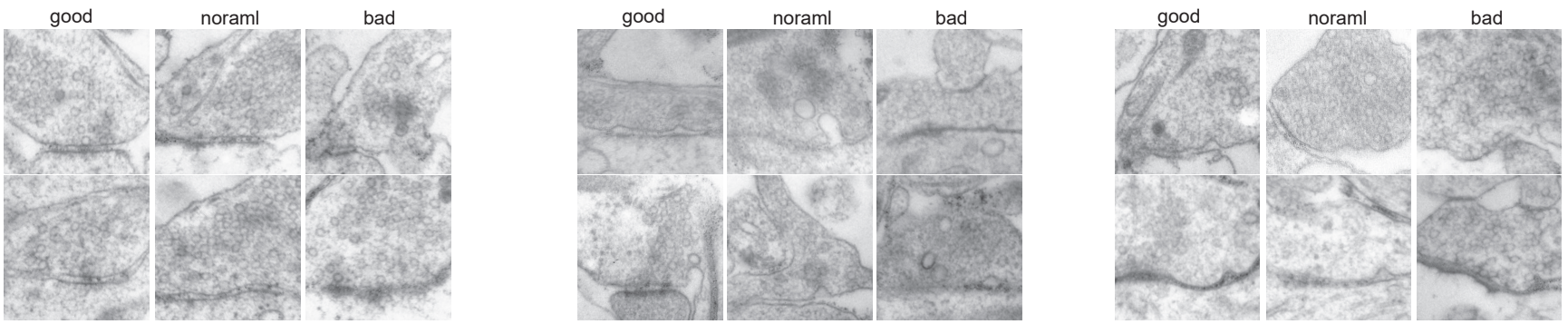

Dyn1,3 DKO
Dyn1xB S774/8A OEx

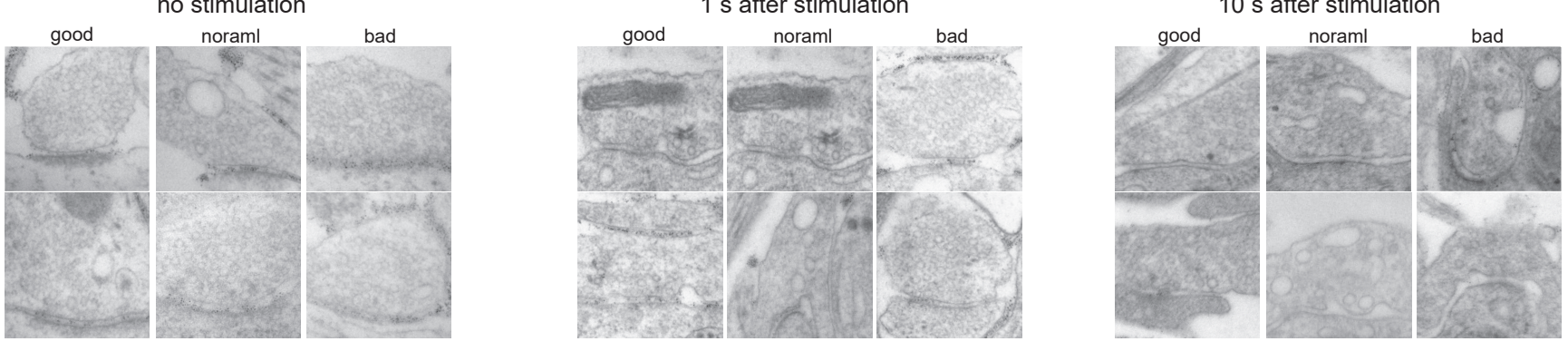

Figure S11. Additional EM images for Figure 1. Related to Figure 1.

Example micrographs showing endocytic pits and ferritin-containing endocytic structures at the indicated time points in *Dyn3* KO, *Dyn1, 3* DKO, *Dyn1, 3* DKO, Dyn1xA overexpression (OEx), *Dyn1, 3* DKO, Dyn1xB OEx, *Dyn1, 3* DKO, Dyn1xB S774/778A OEx. The images are categorized by their qualities (good, normal, and bad). Scale bar: 100 nm.